Positively Charged Nanosheets Derived via Total Delamination of Layered Double Hydroxides

Liang Li, Renzhi Ma, Yasuo Ebina, Nobuo Iyi, and Takayoshi Sasaki*

Advanced Materials Laboratory, National Institute for Materials Science, 1-1 Namiki, Tsukuba, Ibaraki 305-0044, Japan

Received May 17, 2005. Revised Manuscript Received June 28, 2005

Positively charged nanosheets with a lateral dimension of micrometers have been synthesized by directly delaminating a well-crystallized Mg−Al layered double hydroxide (LDH) in the nitrate form. The action of formamide on LDH crystals 10 μm in size led to a transparent solution. X-ray diffraction measurement on a glue-like colloid centrifuged from the solution detected a broad feature at small angular range, while completely losing the sharp reflections for the precursor crystalline compound. The broad profile was very similar to the square of the structure factor calculated based on the LDH structure, which provides strong evidence for the total exfoliation of the LDH crystals into their single sheets. Upon in situ aging in a stream of nitrogen gas, the broad pattern was gradually converted into a sharp basal diffraction pattern, indicating the restacking of molecular LDH nanosheets to restore the original stacked form. Observations by transmission electron microscopy and atomic force microscopy revealed delaminated nanosheets with a lateral size of several micrometers and a thickness of 0.8 nm. The electron diffraction data and elemental microanalysis results as well as these morphological features supported the formation of unilamellar LDH sheets. The LDH nanosheets could be assembled layer-by-layer with an anionic polymer, poly(sodium styrene 4-sulfonate) (PSS), onto the solid surface to produce ultrathin nanocomposite films, demonstrating their usefulness as a positively charged lamellar nanoblock. The formation of nanostructured multilayer assemblies was confirmed by the progressive enhancement of UV absorbance due to PSS and the evolution of X-ray diffraction peaks showing a repeating distance of ∼2.0 nm.

Introduction

Exfoliation of layered host compounds has received increasing attention because the resulting unilamellar crystallites, or nanosheets, have various attractive aspects connected to unusual structural features, that is, ultimate two-dimensional anisotropy. In particular, recent successes in the synthesis of functional oxide nanosheets, e.g., $Ti_{1-\delta}O_2$, MnO_2, and $Ca_2Nb_3O_{10}$, have stimulated significant interest in this new class of nanomaterials.[1−5] The nanosheets exhibit novel physical and chemical properties due to an extremely small thickness of around 1 nm. Furthermore, these nanosheets are useful as a building block for the fabrication of a wide variety of functional nanostructured materials.[6] One of the most important and advanced such examples is the layer-by-layer assembly of nanosheets with appropriately charged counterparts through a wet process.[7−10] Intensive research has been directed to the development of nanodevices through this sophisticated route.[11,12]

Most of the nanosheets synthesized so far are "macroanions" bearing negative charge. Positively charged nanosheets

* Corresponding author. Phone: 81-29-860-4313. Fax: 81-29-854-9061. E-mail: SASAKI.takayoshi@nims.go.jp.

(1) (a) Sasaki, T.; Watanabe, M.; Hashizume, H.; Yamada, H.; Nakazawa, H. *J. Am. Chem. Soc*. **1996**, *118*, 8329. (b) Sasaki, T.; Watanabe, M. *J. Am. Chem. Soc.* **1998**, *120*, 4682. (c) Tanaka, T.; Ebina, Y.; Takada, K.; Kurashima, K.; Sasaki, T. *Chem. Mater*. **2003**, *15*, 3564. (d) Sugimoto, W.; Terabayashi, O.; Murakami, Y.; Takasu, Y. *J. Mater. Chem*. **2002**, *12*, 3814.

(2) (a) Liu, Z. H.; Ooi, K.; Kanoh, H.; Tang, W.-P.; Tomida, T. *Langmuir*, **2000**, *16*, 4154. (b) Omomo, Y.; Sasaki, T.; Wang, L. Z.; Watanabe, M. *J. Am. Chem. Soc*. **2003**, *125*, 3568.

(3) (a) Treacy, M. M. J.; Rice, S. B.; Jacobson, A. J.; Lewandowski, J. T. *Chem. Mater*. **1990**, *2*, 279. (b) Domen, K.; Ebina, Y.; Ikeda, S.; Tanaka, A.; Kondo, J. N.; Maruya, K. *Catal. Today* **1996**, *28*, 264. (c) Schaak, R. E.; Mallouk, T. E. *Chem.* Mater. **2000**, *12*, 3427. (d) Schaak, R. E.; Mallouk, T. E. *Chem. Mater*. **2002**, *14*, 1455. (e) Ebina, Y.; Sasaki, T.; Watanabe, M. *Solid State Ionics* **2002**, *151*, 177.

(4) (a) Takagaki, A.; Sugisawa, M.; Lu, D.; Kondo, J. N.; Hara, M.; Domen, K.; Hayashi S. *J. Am. Chem. Soc*. **2003**, *125*, 5479. (b) Takagaki, A.; Yoshida, T.; Lu, D.; Kondo, J. N.; Hara, M.; Domen, K.; Hayashi S. *J. Phys. Chem. B* **2004**, *108*, 11549.

(5) (a) Abe, R.; Shinohara, K.; Tanaka, A.; Hara, M.; Kondo, J. N.; Domen, K. *J. Mater. Res*. **1998**, *13*, 861. (b) Saupe, G. B.; Waraksa, C. C.; Kim, H.-N.; Han, Y. J.; Kaschak, D. M.; Skinner, D. M.; Mallouk, T. E. *Chem. Mater*. **2000**, *12*, 1556. (c) Miyamoto, N.; Yamamoto, H.; Kaito, R.; Kuroda, K. *Chem. Commun*. **2002**, 2378.

(6) Jacobson, A. J. *Comprehensive Supramolecular Chemistry*; Alberti, G., Bein, T., Eds.; Elsevier Science: Oxford, U.K., 1996; Vol. 7, pp 315−335.

(7) (a) Okamoto, K.; Tamura, K.; Taniguchi, M.; Yamagishi, A. *Colloid Surf., A* **1999**, *169*, 241. (b) Umemura, Y.; Yamagishi, A.; Schoonheydt, R.; Persoons, A.; Schryver, F. D. *J. Am. Chem. Soc*. **2002**, *124*, 992. (c) Yamaki, T.; Asai, K. *Langmuir* **2001**, *17*, 2564.

(8) (a) Kleinfeld, E. R.; Ferguson, G. S. *Science* **1994**, *265*, 370. (b) Kotov, N. A.; Haraszti, T.; Turi, L.; Zavala, G.; Geer, R. E.; Dékány, I.; Fendler, J. H. *J. Am. Chem. Soc*. **1997**, *119*, 6821. (c) Kim, D. W.; Blumstein, A.; Tripathy, S. K. *Chem. Mater*. **2001**, *13*, 1916.

(9) (a) Keller, S. W.; Kim, H.-N.; Mallouk, T. E. *J. Am. Chem. Soc*. **1994**, *116*, 8817. (b) Kim, H.-N.; Keller, S. W.; Mallouk, T. E.; Schmitt, J.; Decher, G. *Chem. Mater*. **1997**, *9*, 1414. (c) Fang, M.; Kim, C. H.; Saupe, G. B.; Kim, H.-N.; Waraksa, C. C.; Miwa, T.; Fujishima, A.; Mallouk, T. E. *Chem. Mater*. **1999**, *11*, 1526. (d) Schaak, R. E.; Mallouk, T. E. *Chem. Mater*. **2000**, *12*, 2513.

(10) (a) Sasaki, T.; Ebina, Y.; Tanaka, T.; Harada, M.; Watanabe, M.; Decher, G. *Chem. Mater*. **2001**, *13*, 4661. (b) Wang, L. Z.; Omomo, Y.; Sakai, N.; Fukuda, K.; Nakai, I.; Ebina, Y.; Takada, K.; Watanabe, M.; Sasaki, T. *Chem. Mater*. **2003**, *15*, 2873. (c) Wang, L. Z.; Ebina, Y.; Takada, K.; Sasaki, T. *J. Phys. Chem. B* **2004**, *108*, 4283. (d) Wang, L. Z.; Sakai, N.; Ebina, Y.; Takada, K.; Sasaki, T. *Chem. Mater*. **2005**, *17*, 1352.

10.1021/cm0510460 CCC: $30.25
Published on Web 07/29/2005

are expected to further widen the applicability and flexibility in materials synthesis using two-dimensional nanomaterials. For this purpose, considerable attention has been paid to layered double hydroxides (LDHs, with a general formula of $[M^{2+}_{1-x}M^{3+}_{x}(OH)_2][A_n^{-x/n}\cdot mH_2O]$), consisting of positively charged brucite-like layers and charge-balancing interlayer anions.[13,14] However, a high charge density of LDH layers associated with a high content of guest anions results in strong interlayer electrostatic interactions,[15] which makes it difficult to exfoliate the LDHs via normal procedures. Several groups attempted to delaminate the LDHs in nonaqueous solvents after replacing interlayer inorganic anions with organophilic anions, e.g., fatty acid salts or anionic surfactants, which substantially modifies the surface properties and weakens interlayer interactions.[16−18] Adachi-Pagano et al. reported that delamination may occur by refluxing Zn−Al dodecyl sulfate LDHs with alcohols at 120 °C.[16] Hibino and Jones reported an exfoliation procedure involving the intercalation of amino acids and the subsequent treatment with formamide.[17] The LDHs that have been used in these exfoliation experiments were prepared by a conventional coprecipitation method involving hydrolysis with NaOH or NH_3. The materials obtained through this route were composed of very small crystallites, usually several tens of nanometers in lateral size, and often in an aggregated form of heavily buckled fine crystallites. From this reason, exfoliated products were difficult to characterize. This has sometimes limited applications of the delaminated sheets. Furthermore, the multistep processes reported were complicated and time-consuming.

Recently, the synthesis of large Mg−Al LDH crystals has been demonstrated by using urea or hexamethylenetetramine as a hydrolysis agent.[19,20] The present paper reports on the delamination of these large crystals via a simple procedure. We found that the only treatment of the nitrate LDH with formamide at room temperature yielded colloidal LDH nanosheets having a lateral size of several micrometers. The complete exfoliation was clearly evidenced by various characterization techniques. These results will open up new application fields for the LDHs. The layer-by-layer self-assembly of the LDH nanosheets and anionic polymers to produce multilayer nanocomposite films was demonstrated as one such example.

Experimental Section

Reagents and Materials. The chemicals used were of reagent grade or higher purity. Milli-Q filtered water was used throughout the experiments. Poly(sodium 4-styrene sulfonate) (PSS) and polyethylenimine (PEI, 50 wt % aqueous solution) were purchased from Aldrich Co. and used without further purification. The molecular weight is $\sim 7 \times 10^4$ for PSS and $\sim 7.5 \times 10^5$ for PEI.

The precursor of the Mg−Al LDH crystals was synthesized by the procedure reported recently.[20] Chemicals such as $Mg(NO_3)_2\cdot 6H_2O$ (0.02 mol), $Al(NO_3)_3\cdot 9H_2O$ (0.01 mol), and hexamethylenetetramine (0.026 mol) were mixed together and dissolved into an aqueous solution of 80 cm^3. The mixture was placed in an autoclave and heated at 140 °C for 24 h. The obtained material was recovered by filtration, washed with water, and dried in air. This sample of 0.5 g was further treated with 500 cm^3 of an aqueous solution containing $NaNO_3$ (0.75 mol) and HNO_3 (0.0025 mol) to expel interlayer carbonate ions. The reaction vessel was tightly capped after purging with nitrogen gas, and was shaken for 1 day at ambient temperature. The sample was recovered by centrifugation, washed with water, and vacuum-dried.

Exfoliation of Nitrate Mg−Al LDH. An amount of 0.05 g of the LDH sample was mixed with 100 cm^3 of formamide in a flask, which was tightly sealed after purging with nitrogen gas. The mixture was vigorously agitated by a mechanical shaker at a speed of 170 rpm.

Fabrication of Multilayer Films. Multilayer ultrathin films of the LDH nanosheets were fabricated by applying the LBL assembly procedure similar to that described previously.[10] Substrates, such as a Si wafer and a quartz glass slide, were cleaned by treatment in a bath of methanol/HCl (1/1 v/v) and then concentrated H_2SO_4 for 20 min each. The substrate was immersed in an aqueous solution of PEI (1.25 g dm^{-3}, pH = 9) for 20 min, followed by rinsing with a copious amount of water. The substrate thus primed with PEI was treated with a PSS aqueous solution (1 g dm^{-3}) for 20 min and washed with water. The conditions employed here have been established to coat the substrate surface with a monolayer of corresponding polyelectrolytes.[10] The substrate was then dipped in a colloidal suspension (0.5 g dm^{-3}) of LDH nanosheets for 20 min and washed with water again. The series of deposition operations for the PSS and LDH nanosheets was repeated *n* times to produce multilayer films of $(PSS/LDH)_n$. The resulting films were dried with a nitrogen gas flow.

Characterizations. Chemical analyses of starting LDHs were carried out as follows. The Mg and Al contents were determined by ICP atomic emission spectroscopy (SEIKO SPS1700HVR) after dissolving a weighed amount of sample with an HCl solution. The carbonate content was obtained by integrating the IR signal of CO_2 evolved in the heating process (LECO RC-412). The water content was deduced from ignition loss data at 1000 °C.

X-ray diffraction (XRD) data were collected by a Rigaku Rint-2000 diffractometer with a graphite-monochromatized Cu Kα radiation ($\lambda = 0.15405$ nm). A specially designed diffractometer (Rigaku Rint-2000S) equipped with a horizontal goniometer stage and a closed sample chamber was employed for measurements where drying of a wet sample needs to be controlled.

UV−vis absorption spectra for the multilayer films were recorded in transmission mode using a Hitachi U-4000 spectrophotometer.

(11) Mallouk, T. E.; Gavin, J. A. *Acc. Chem. Res.* **1998**, *31*, 209.
(12) Cassagneau, T.; Fendler, J. H.; Johnson, S. A.; Mallouk, T. E. *Adv. Mater.* **2000**, *12*, 1363.
(13) (a) Ingram, L.; Taylor, H. F. W. *Mineral. Mag.* **1967**, *36*, 465. (b) Allmann, R. *Acta Crystallogr., Sect. B* **1968**, *24*, 972.
(14) Roy, A.; Forano, C.; Malki, K. E.; Besse, J.-P. Anionic Clays: Trends in Pillaring Chemistry; In *Synthesis of Microporous Materials*; Occelli, M. L., Robson, H. E., Eds.; Van Nostrand Reinhold: New York, 1992.
(15) Albiston, L.; Franklin, K. R.; Lee, E.; Smeulders, J. B. A. F. *J. Mater. Chem.* **1996**, *6*, 871.
(16) (a) Adachi-Pagano, M.; Forano, C.; Besse, J.-P. *Chem. Commun.* **2000**, 91. (b) Leroux, F.; Adachi-Pagano, M.; Intissar, M.; Chauvière, S.; Forano, C.; Besse, J.-P. *J. Mater. Chem.* **2001**, *11*, 105.
(17) (a) Hibino, T.; Jones, W. *J. Mater. Chem.* **2001**, *11*, 1321. (b) Hibino, T. *Chem. Mater.* **2004**, *16*, 5482.
(18) O'Leary, S.; O'Hare, D.; Seeley, G. *Chem. Commun.* **2002**, 1506.
(19) (a) Cai, H.; Hillier, A. C.; Franklin, K. R.; Nunn, C. C.; Ward, M. D. *Science* **1994**, *266*, 1551. (b) Costantino, U.; Coletti, N.; Nocchetti, M.; Aloisi, G. G.; Elisei, F. *Langmuir* **1999**, *15*, 4454. (c) Costantino, U.; Marmottini, F.; Nocchetti, M.; Vivani, R. *Eur. J. Inorg. Chem.* **1998**, 1439. (d) Yao, K.; Taniguchi, M.; Nakata, M.; Takahashi, M.; Yamagishi, A. *Langmuir* **1998**, *14*, 2410. (e) Ogawa, M.; Kaito, H. *Langmuir* **2002**, *18*, 4240. (f) Adachi-Pagano, M.; Forano, C.; Besse, J.-P. *J. Mater. Chem.* **2003**, *13*, 1988.
(20) (a) Iyi, N.; Matsumoto, T.; Kaneko, Y.; Kitamura, K. *Chem. Lett.* **2004**, *33*, 1122. (b) Iyi, N.; Matsumoto, T.; Kaneko, Y.; Kitamura, K. *Chem. Mater.* **2004**, *16*, 2926.

Transmission electron microscope (TEM) observations were performed on a field emission JEM-3000F (JEOL) electron microscope operated at 300 kV and equipped with a Gatan-666 electron energy loss spectrometer and energy-dispersive X-ray spectrometer.

Scanning electron micrographs (SEM) were obtained using a JEOL JSM-6700F electron microscope (accelerating voltage of 10 kV).

A Seiko SPS-1100 atomic force microscope (AFM) instrument was employed to obtain a topographical image of the nanosheets. Samples were prepared by adsorbing the nanosheets from a suspension onto a Si wafer precoated with double layers of polymers such as PEI and PSS. The deposition conditions were the same as those used for the synthesis of the multilayer films. Measurements were carried out in tapping mode with silicon-tip cantilevers (14 N m^{-1}).

Results and Discussion

Exfoliation Behavior. Highly crystalline Mg−Al LDHs were synthesized according to a reported procedure[20] and were employed as a starting precursor for the nanosheets. XRD data (see the Supporting Information) and FT-IR absorption spectra agreed well with the previous report. Chemical analysis for the as-prepared sample indicated a composition of $[Mg_{0.65}Al_{0.33}(OH)_2][(CO_3)_{0.17}\cdot 0.5H_2O]$ (Anal. Calcd: Mg, 20.3%; Al, 11.4%; C, 2.6%; ignition loss, 44.8%. Found: Mg, 20.4%; Al, 11.6%; C, 2.6%; ignition loss 45.1%). The composition obtained is typical for LDHs in the carbonate form.[14,19c] After reaction with an aqueous solution of $NaNO_3$ + HNO_3, a gallery height of 0.89 nm was obtained (Figure 1a), confirming the formation of the nitrate form of the LDH. The atomic ratio of Mg/Al was 1.91, indicating no appreciable change of the LDH host during the ion exchange process. An SEM image revealed uniform crystals, hexagonal in shape, with a large lateral dimension of about 10 μm, as shown in Figure 2. A TEM image and electron diffraction data (see the Supporting Information) also demonstrate the well-crystallized LDHs.

Treatment of these large LDH crystals with formamide at room temperature yielded an apparently transparent solution after vigorous shaking for 12 h, and no sediment was observed upon standing. To explore the colloidal state of the LDH sample, the suspension was centrifuged for 20 min at a speed of 30 000 rpm to separate a colloidal material dispersed from the solvent of formamide. The colloidal aggregate having a glue-like appearance was recovered. Its XRD data recorded without drying is depicted in Figure 1b (top) together with the blank data for formamide itself (bottom). Both patterns exhibited a pronounced halo in a 2θ range of 20−30°, which may be ascribed to the scattering of liquid formamide. One of the most striking features for the paste-like sample is the absence of sharp basal peaks. This suggests that the host sheets are not in parallel to induce interference of the X-rays, implying exfoliation. Instead, a broad component (indicated by an arrow) was recognized in a very low angular region when compared with the blank data.

We have demonstrated that colloidal materials centrifuged from suspensions of exfoliated layered hosts, such as $H_{0.7}Ti_{1.825}\square_{0.175}O_4\cdot H_2O$ (□: vacancy), $H_{0.13}MnO_2\cdot 0.7H_2O$, and

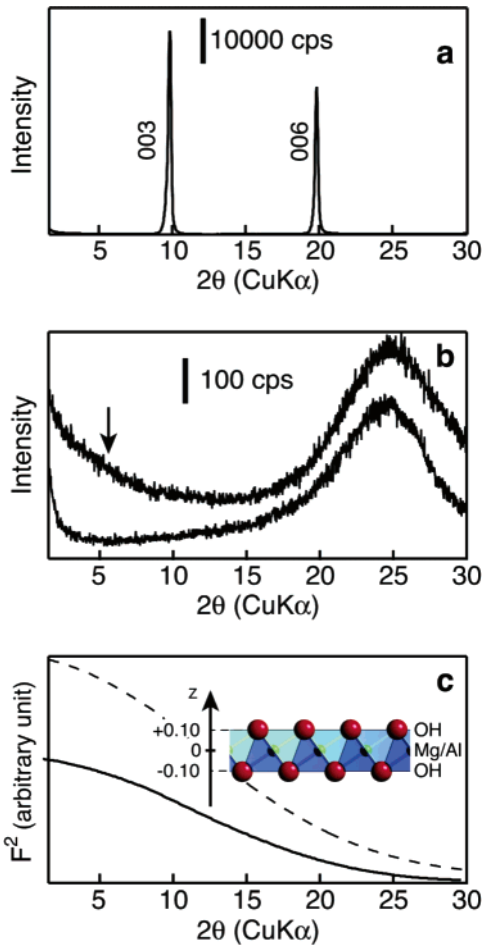

Figure 1. (a) XRD pattern of starting LDH. (b) XRD pattern for the colloidal aggregate centrifuged from the suspension (top). The bottom trace denotes the blank data for formamide itself. (c) Square of the structure factor of the Mg−Al LDH sheet (solid trace). Comparable data for the MnO_2 nanosheet is shown as a dotted trace. The inset represents the structure of the LDH sheet.

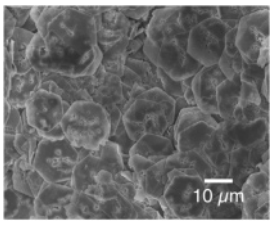

Figure 2. SEM image of LDH crystals after ion exchange treatment. Some etched pits in the crystals may have formed during the ion exchange process using the acidic solution.

$HCa_2Nb_3O_{10}\cdot 1.5H_2O$, exhibited a broad diffraction pattern, losing sharp reflections attributable to the corresponding layered structure.[1b,2b,3e] More importantly, the profile is characteristic of the layered material exfoliated, representing close similarities to the square of the structure factor of the host layer. This has been taken as compelling evidence for total exfoliation, because the square of the structure factor should correspond to the pattern arising from scattering of individual sheets. This X-ray analysis should be reliable because the signal is collected from a macroscopic amount of sample, in contrasting to the electron microscope data from a very limited field.

In this line, we calculated the structure factor of the LDH sheet based on a composition of $Mg_{2/3}Al_{1/3}(OH)_2$ and its well-

known hexagonal structure (inset in Figure 1c) as follows:

$$F = f_{Mg/Al} + 2f_{OH} \cos 2\pi \cdot 2z \cdot \sin \theta/\lambda \quad (1)$$

where $f_{Mg/Al}$ and f_{OH} are the mean atomic scattering factors for virtual species, such as $^2/_3$Mg + $^1/_3$Al and O + H, and θ and λ are the diffraction angle and wavelength of the X-ray, respectively. Because the sheet is centrosymmetric with respect to the *xy* plane, only the cosine term is taken into consideration. The position of OH was set to $z = 0.10$ nm on the basis of reported Rietveld refinement results on Mg−Al LDHs.[19c,21] The calculated profile (the solid trace in Figure 1c) is similar to the broad component observed, verifying the total and complete delamination of the LDH sample.

The simple architecture of the LDH sheet along its normal line, where the metal ion is sandwiched with OH groups, is responsible for the less conspicuous intensity distribution of monotonically decreasing profile. As reported previously,[2b] MnO_2 nanosheets have an intensity profile (dotted trace in Figure 1c) similar to that for LDH sheets because the essential layer architecture is in common, the only differences being Mn or Mg/Al, and O^{2-} or OH^- in the sheets. A contrasting case can be found in the $Ca_2Nb_3O_{10}$ nanosheet, which shows a characteristic oscillating profile.[3e] The thickness of this nanosheet is composed of triple NbO_6 octahedra which are corner-shared with each other.

It should be emphasized that the delamination was achieved directly by starting from the nitrate LDH. In previous reports,[16−18] delamination was attained only after the interlayer gallery was modified with organic guests such as fatty acid salts or amino acids. Hibino and Jones pointed out in their report of delamination of LDHs modified with glycine in formamide that the interaction between interlayer glycine and formamide is particularly important.[17a] Most recently, Hibino reported that the LDHs containing a very small amount of amino acids (less than 1% of the anion exchange capacity) can be delaminated with formamide.[17b] Our results may be taken as its extreme limit, but another explanation for the delamination mechanism is necessary because the LDH gallery in our sample does not contain amino acids. It is well-known that there is a dense network of hydrogen bonds in the interlayer space of LDHs; interlayer water molecules are hydrogen-bonded to hydroxyl groups of the LDH host and, at the same time, are coordinated to interlayer anionic guests.[22] Because formamide is highly polar, its carbonyl group would have a strong interaction to the LDH host, replacing the interlayer water molecules. The other end of the formamide molecule, NH_2, may not be able to build a strong bonding to the interlayer anions. Accordingly, once the replacement of water molecules for formamide takes place, it weakens the interlayer attraction force through the destruction of the strong hydrogen-bonding network and induces delamination.

The success of delamination without interlayer modification is beneficial by saving additional chemical treatment and time. In addition, large-sized LDH crystals can be employed as a precursor, which can yield well-defined nanosheets in large dimensions. It is generally difficult to incorporate bulky guest species into larger crystals. This may be one of the main reasons why LDHs employed in the previous delamination studies have been synthesized via coprecipation methods with NaOH as a hydrolyzing agent, which usually produces LDHs with a submicrometer or smaller size. For example, LDHs containing amino acids were prepared by adding a mixed solution of $Mg(NO_3)_2$ + $Al(NO_3)_3$ to a NaOH solution of amino acids.

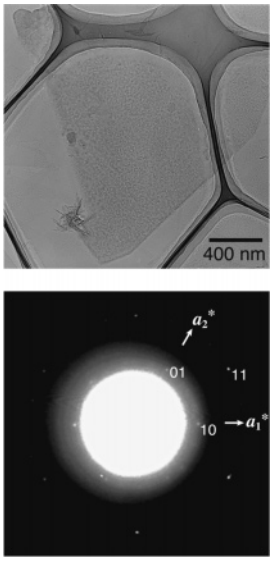

Figure 3. TEM image of the LDH nanosheet (top) and its selected area diffraction pattern (bottom).

Characterization of LDH Nanosheets. TEM and AFM observations further confirmed the delamination, visualizing the morphology of the obtained LDH nanosheets. A typical TEM image (Figure 3a) shows two-dimensional objects, which can be identified as the delaminated LDH sheets. Their very faint but uniform contrast is compatible with the ultrathin thickness of the crystallites. The ultrafaint contrast should be expected for the single LDH sheet, and it is difficult to conclude if the observed contrast is compatible with that. When its extreme weakness is taken into account, it may be of a few stacked sheets at most. Note that the image could be taken only by using an unusual defocus condition (>1 μm) to signify the nanosheet contrast, which is again ascribed to the ultrathin nature of the crystallites. The LDH nanosheets obtained in this study had a lateral size, usually >1 μm, which is very large and well-defined in comparison to the "nanosized LDH nanosheets" reported so far,[16−18] although the loss of hexagonal shape as well as the size reduction in comparison with the original LDH crystals indicates the fracture or breakage of the sheets during the delamination to some extent.

EDX analysis detected Mg, Al, and O from the LDH nanosheet as well as C and Cu derived from a supporting TEM grid. The Mg/Al ratio for the sheets was 1.6 on average, which is close to that (1.91) of the starting precursor crystals. The small difference may imply some dissolution of metal ions during the process, and further study on this point will be needed.

(21) Bellotto, M.; Rebours, B.; Clause, O.; Lynch, J.; Bazin, D.; Elkaïm, E. *J. Phys. Chem.* **1996**, *100*, 8535.
(22) Wang, J. W.; Kalinichev, A. G.; Amonette, J. E.; Kirkpatrick, R. J. *Am. Mineral.* **2003**, *88*, 398.

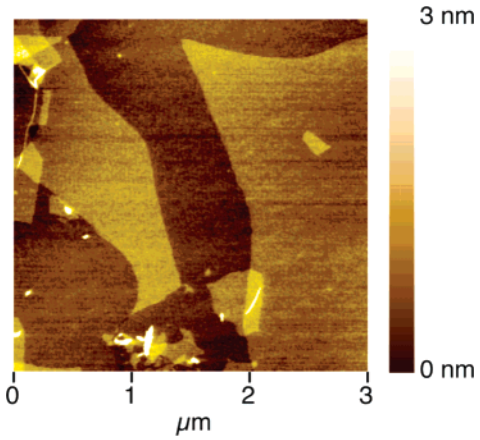

Figure 4. Tapping mode AFM image of delaminated LDH sheets deposited on a Si wafer substrate.

The selected-area electron diffraction pattern was comprised of hexagonally arranged spots (Figure 3b),[23] although they tended to change into arcs or rings during the observation. This may be due to the beam sensitivity of the sample, because the hydroxides are expected to be less stable in an ultrahigh vacuum atmosphere. The cell parameter of the two-dimensional hexagonal unit cell measured from the electron diffraction pattern was $a = 0.31$ nm, which is in acceptable agreement with the in-plane structural parameter of Mg−Al LDH crystals ($a = 0.305$ nm) in view of the accuracy of electron diffraction data.

A tapping-mode AFM image (Figure 4) revealed sheetlike objects with a similar lateral size as those detected by TEM observations, although fragments were also occasionally observed. The height profile scan indicated that the crystallite terrace was fairly flat. The thickness was measured at steps between a nanosheet and a substrate surface and between a nanosheet and another overlapped on it. The data collected from over 10 different spots yielded an average value of 0.81 ± 0.05 nm for the former and 0.78 ± 0.02 nm for the latter. The small standard deviation indicated a unique thickness of the sheet. The theoretical thickness of the LDH sheet is 0.48 nm.[14,17] Possible adsorption of formamide as well as counteranions, e.g., NO_3^- or CO_3^{2-}, on the nanosheet surface may be responsible for the deviation of ~0.30 nm, or the van der Waals radius of hydrogen atoms (0.12 nm) may account for it. In any case, the thickness observed obviously indicates that the sheets are unilamellar.

Restacking Behavior of LDH Nanosheets. The colloidal LDH nanosheets underwent restacking upon aging under a nitrogen gas stream, which was monitored by XRD data (Figure 5). The colloidal aggregate centrifuged from the suspension only showed the broad pattern arising from the LDH nanosheets and formamide, as described above. A diffraction series showing a basal spacing of ~1.2 nm (designated by circles) emerged immediately after the initiation of aging. In addition to this major basal series, there was a small peak at a 2θ of 2.8° (shown by an arrow on trace c), suggesting the presence of a highly swollen phase

(23) The intensity of the diffraction spots were much weaker than those for the original LDHs before exfoliation. Furthermore, the beam sensitivity of the LDH crystals was not very significant. These features are again due to the ultrathin nature of the delaminated sheets.

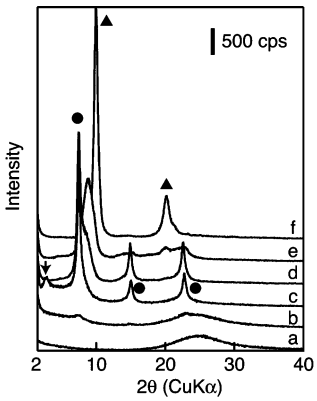

Figure 5. Evolution of the XRD profile starting from the colloidal aggregate of LDH nanosheets; (a) start of aging, (b) after 1 day, (c) 3 days, (d) 5 days, (e) 7 days, and (f) 10 days. Symbols such as circles and triangles denote the basal diffraction series with a spacing of 1.2 and 0.9 nm, respectively.

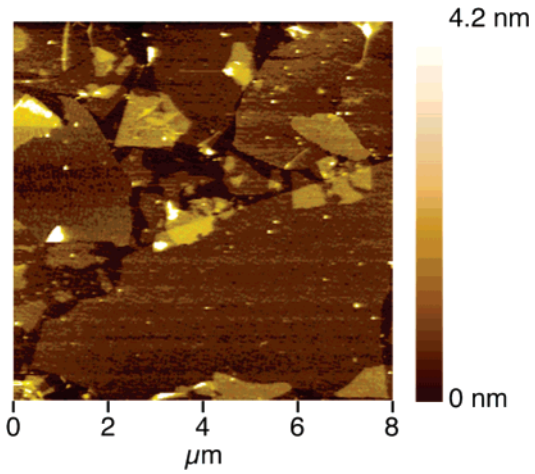

Figure 6. AFM image of the first LDH nanosheet layer on a Si wafer precoated with PEI and PSS; nanosheet concentration, 0.5 g dm^{-3}.

($d \sim 3.2$ nm). This may be comparable to the largely expanded phases that appeared in the reassembling processes of oxide nanosheets[1b,2b] such as $Ti_{0.91}O_2$ and MnO_2.

The 1.2 nm phase increased in abundance with time, accompanied by the disappearance of the highly swollen phase as well as the broad profile. This process can be understood in terms of restacking of LDH nanosheets, namely, from nanosheets as a molecular entity to lamellar aggregates as a one-dimensional crystal, which is promoted by evaporation of formamide. An FT-IR spectrum (see the Supporting Information) indicates that the nitrate ion, which was present in the LDH crystals before exfoliation, is a major anionic guest in the restacked material. The large basal spacing of 1.2 nm may be explained by the cointercalation of formamide into the LDH gallery. In prolonged aging over 5 days, the cointercalated formamide was eventually removed and the original nitrate form with a basal distance of 0.90 nm (denoted by triangles) was restored.

Layer-by-Layer Assembly of Composite Films with PSS. Figure 6 depicts a typical AFM image displaying the surface topography after dipping a Si wafer substrate precoated with PEI/PSS bilayers in the colloidal suspension of exfoliated LDH nanosheets. PEI and PSS themselves were not perceptible. The substrate surface was densely tiled with the LDH nanosheets with a lateral size ranging from

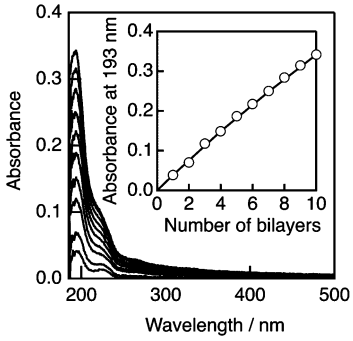

Figure 7. UV−vis absorption spectra of multilayer films of $(PSS/LDH)_n$ prepared on a quartz glass substrate precoated with PEI; nanosheet concentration, 0.5 g dm^{-3}; deposition time, 20 min.

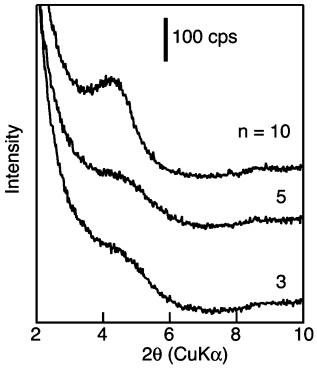

Figure 8. XRD pattern for the multilayer assembly of $(PSS/LDH)_n$ on a quartz glass slide.

hundreds of nanometers to several micrometers. This effective coverage onto the negatively charged surface indicates that the LDH nanosheets are positively charged. Although there were some overlaps and uncovered gaps, the monolayer region was predominant. The overall coverage was determined to be 88%, and the overlapped percentage was 11%. The coverage was similar to that for ultrathin films fabricated with oxide nanosheets, $Ti_{0.91}O_2$ and MnO_2, and organic polyelectrolytes.[9,10] The overlapped patches were relatively limited, probably because of the larger lateral size of the LDH sheets in comparison with the oxide sheets.

The growth of PSS/LDH multilayer films under the optimized conditions was monitored by UV−vis absorption spectra (Figure 7) measured immediately after each deposition cycle. An absorption band around 200 nm is diagnostic of PSS. The nearly linear increment of its absorbance indicates the successful LBL assembly of multilayer ultrathin films of LDH nanosheets and PSS. An absorbance of 0.34 at 193 nm was reached after the deposition of 10 bilayers. This value was comparable to that for a multilayer film of $(PSS/PDDA)_{10}$ (PDDA = polydiallydimethylammonium chloride),[24] demonstrating again that the LDH nanosheets are as effective as organic linkers serving as a positively charged nanomodule. To the best of our knowledge, this is the first report on the LBL assembly of LDH nanosheets and an anionic polymer to produce molecularly organized films.

The multilayer ultrathin films of $(PSS/LDH)_n$ exhibited a Bragg peak at a 2θ value of 4.4°, indicating a spacing of ~2.0 nm (see Figure 8). Although it was broad, its intensity was enhanced with the increasing number of deposition cycles, and the second-order peak ($2\theta \sim 8.6°$) became barely resolved for the thicker films. This diffraction feature is attributable to a repeating periodicity of bilayers of inorganic LDH nanosheets and organic polymer, and its enhancement with increasing numbers of deposition cycles indicates the progressive growth of its nanostructured assemblies. A similar gallery height of 2.08 nm was reported for a nanocomposite of LDH/PSS synthesized via the in situ coprecipitation method.[25]

If we take 0.48 nm as a thickness of the LDH nanosheets, the remaining height of 1.5 nm may be for the PSS layer. Recently the height of PSS molecules on a positively charged surface has been reported to be 0.5−1.0 nm.[26] The difference may be accounted for by a different configuration of PSS on the nanosheets and/or the presence of water molecules or formamide.

Conclusion

The interaction of formamide with Mg−Al LDH crystals 10 μm in size promoted the total delamination to yield colloidal LDH nanosheets. The nitrate LDH could be directly delaminated, and no pretreatment was required. The characterizations by XRD, TEM, and AFM provided undisputable evidence for the formation of the unilamellar LDH nanosheets, which were as large as several micrometers in lateral size. Because they are one of the first well-defined positively charged nanosheets, we can expect various applications, including the fabrication of nanostructured materials and systems, by using them as building blocks.

Acknowledgment. This study was supported by CREST of the Japan Science and Technology Agency (JST).

Supporting Information Available: XRD, TEM image, and electron diffraction data of LDH crystals used as a precursor of the nanosheets; FT-IR spectrum for the restacked LDH nanosheets obtained by aging in nitrogen gas. This material is available free of charge via the Internet at http://pubs.acs.org.

CM0510460

(24) Zeng, T.; Claus, R.; Liu, Y.; Zhang, F.; Du, W.; Cooper, K. L. S*mart Mater. Struct.* **2000**, *9*, 801.

(25) Oriakhi, C. O.; Farr, I. V.; Lerner, M. M. *J. Mater. Chem.* **1996**, *6*, 103.

(26) Zhu, M.; Schneider, M.; Papastavrou, G.; Akari, S.; Möhwald, H. *Langmuir* **2001**, *17*, 6471.